ASCE

Physical Properties, Longitudinal Tensile Properties, and Bond Strength of the New Generation of GFRP Bars

Brahim Benmokrane, M.ASCE[1]; Shehab Mehany[2]; Carol Shield[3]; Antonio Nanni, F.ASCE[4]; and Vicki Brown, M.ASCE[5]

Abstract: This paper presents an experimental study that investigated the physical properties, longitudinal tensile properties, and bond strength of a new generation of glass fiber–reinforced polymer (GFRP) bars. Five commercially available types of GFRP bars with different surface treatments (deformed/ribbed, helically deformed, helically grooved, double helical wrap/sand-coated, and sand-coated) were selected for this investigation. Two bar sizes (No. 5 and No. 8)—with 15.9 and 25.4 mm nominal diameters representing the range of GFRP-reinforcing bars typically used in practice as longitudinal reinforcement in concrete flexural members—were selected from each of the manufacturers. The test results reveal that these new higher modulus GFRP bars have physical properties, tensile strength, and moduli of elasticity greatly exceeding the requirements of ASTM and Canadian Standards Association (CSA) standards. The GFRP bars had measured cross-sectional areas near or slightly over the maximum cross-sectional area allowed by ASTM standards. The mechanical properties reported in this study were based on nominal cross-sectional areas. The longitudinal tensile properties and bond strength of the GFRP bars satisfied the limits in ASTM and CSA standards. GFRP bar manufacturers have developed and are producing GFRP bars with guaranteed strengths that significantly exceed the ASTM minimum specifications. However, ASTM bases qualification methods for tensile strength on the minimum ASTM specified values, which could differ from the values implemented in the design. Until ASTM bases rejection on the strength used in design, the designer should add rejection criteria to the project specifications to ensure that GFRP bar acceptance is based on the strength assumed for design, which could be between the minimum value specified in ASTM and the manufacturer's guaranteed value. **DOI: 10.1061/JCCOF2.CCENG-4300**.

Author keywords: Glass fiber–reinforced polymer (GFRP) bars; Surface treatment; Physical properties; Tensile properties; Bond strength; Reinforced concrete; Material specifications.

Introduction

Glass fiber–reinforced polymer (GFRP) bars are now deemed an acceptable alternative to traditional steel bars as an effective solution to the corrosion problems encountered in reinforced concrete (RC) elements (ACI 440.11-22, ACI 2022). As a result, the number of GFRP bar manufacturers has increased to meet demand, but each company produces GFRP bars with slightly different diameters and significantly different surface treatments. Early studies on the older generations of GFRP indicated that the bars had a lower modulus of elasticity than the new generation of bars and lower durability with a high tendency to alkaline corrosion (Uomoto and Katsuki 1995; Benmokrane and Rahman 1998; Tannous and Saadatmanesh 1999; Benmokrane et al. 2002; Uomoto 2003; Micelli and Nanni 2004). With advancements in manufacturing processes, improved properties of GFRP bar constituent materials, and a higher glass fiber mass fraction, the latest generation of GFRP bars have higher physical and mechanical properties (e.g., GFRP bars with a modulus of elasticity greater than 60,000 MPa are commercially available).

The material properties of the latest generation of GFRP bars are significantly different from the bars that were commercially available when ASTM D7957 was first published. This paper documents the physical, material, and bond characteristics of this new generation of GFRP bars and discusses issues that are pertinent to the design of GFRP-RC when using these bars.

Experimental Program

Materials

GFRP bars from five different manufacturers and with different surface types were selected for use in this investigation. The GFRP bars, as shown in Figs. 1 and 2, are referred to as GFRP1, GFRP2, GFRP3, GFRP4, and GFRP5 for deformed/ribbed, helically deformed, helically grooved, double helical wrap/sand-coated, and sand-coated, respectively. The five GFRP bar types tested were manufactured with a pultrusion process using E-CR (corrosion resistant E-glass) glass fibers impregnated with a vinyl-ester resin in

[1]Professor of Civil Engineering and Tier 1 Canada Research Chair Professor in Advanced Composite Materials for Civil Structures and Industrial Chair Professor in FRP Reinforcement for Concrete Structures, Dept. of Civil and Building Engineering, Univ. of Sherbrooke, Quebec, Canada J1K 2R1. Email: brahim.benmokrane@usherbrooke.ca

[2]Postdoctoral Fellow, Dept. of Civil and Building Engineering, Univ. of Sherbrooke, Quebec, Canada J1K 2R1. Email: shehab.mehany@usherbrooke.ca

[3]Professor Emeritus, Dept. of Civil, Environmental, and Geo-Engineering, Univ. of Minnesota, MN 55455. ORCID: https://orcid.org/0000-0002-8096-8489. Email: ckshield@umn.edu

[4]Professor, Dept. of Civil and Architectural Engineering, Univ. of Miami, FL 33146. ORCID: https://orcid.org/0000-0003-2678-9268. Email: nanni@miami.edu

[5]Distinguished University Professor, Dept. of Civil Engineering, Widener Univ., Chester, PA 19013 (corresponding author). ORCID: https://orcid.org/0000-0002-8738-8559. Email: vlbrown@widener.edu

Note. This manuscript was submitted on March 1, 2023; approved on July 11, 2023; published online on September 25, 2023. Discussion period open until February 25, 2024; separate discussions must be submitted for individual papers. This paper is part of the ***Journal of Composites for Construction***, © ASCE, ISSN 1090-0268.

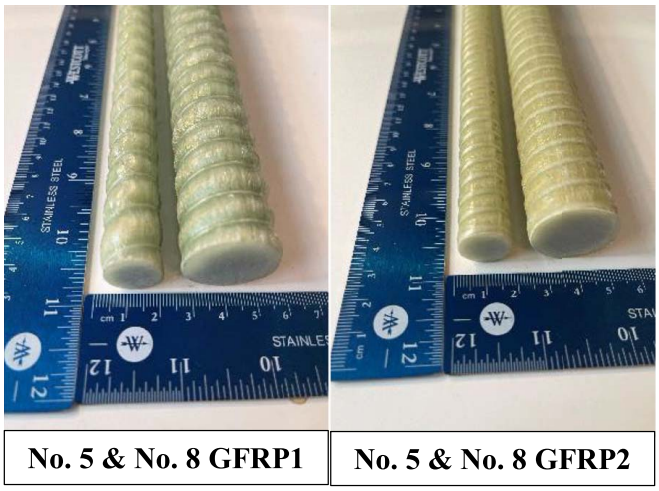

Fig. 1. Identification of the No. 5 and No. 8 GFRP bars tested in this study.

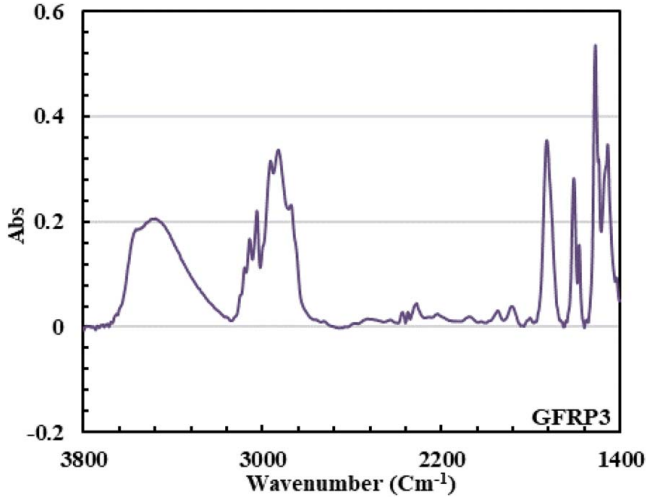

Fig. 3. Typical FTIR spectra of the vinyl-ester resin.

accordance with ASTM D7957-22 (ASTM 2022a) and CSA S807-19 (CSA 2019). In addition, Fourier transform infrared (FTIR) spectroscopy was used to assess the makeup of the resin of the GFRP bars in accordance with CSA S807-19 (CSA 2019). FTIR spectra were recorded using a Jasco 4600 FTIR spectrometer equipped with a diffused reflectance device. Fig. 3 shows the typical FTIR spectra of the resin. Moreover, the chemical composition of the E-CR glass fibers was determined by X-ray fluorescence. Table 1 shows the typical chemical composition of the glass fiber. Two diameters of GFRP bars were investigated (No. 5 and No. 8), which correspond to nominal diameters of 15.9 and 25.4 mm, respectively (Fig. 1). The selected bar sizes represent the range of GFRP-reinforcing bars typically used in research and practice as longitudinal reinforcement in concrete members subjected to bending. Bars from all five manufacturers had modulus of elasticity values in excess of 60 GPa per the manufacturers' data sheets, well in excess of the 44.8 GPa requirement of ASTM D7957-22 (ASTM 2022a). Additionally, two sizes (No. 15 and 25 M) of deformed steel bars were selected in this investigation with nominal diameters of 16 and 25.2 mm, respectively, and nominal cross-sectional areas of 200 and 500 mm^2.

Characterization of the Surface Roughness of GFRP Bars Using a Digital Microscope

Because there are no generally accepted methods to consider the surface variations of different GFRP bars, a digital microscope (KEYENCE Model VHX-7000VHX-7000) was used to investigate the surface profiles of the GFRP bars. The main purpose of microscopic observation is to qualitatively analyze size, shape, and distribution of the surface deformations. This microscope represents a new era of digital microscopy, displaying surface topography

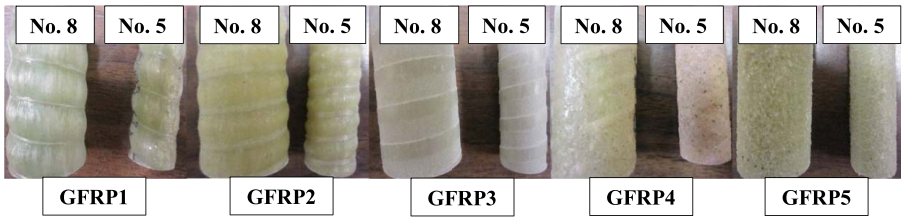

Fig. 2. Close-up view of surface characteristics of the No. 5 and No. 8 GFRP bars.

J. Compos. Constr., 2023, 27(6): 04023056

Table 1. Typical chemical composition of the glass fiber

Chemical	Weight (%)
SiO_2	60.9
CaO	22.5
Al_2O_3	12.5
MgO	2.6
Fe_2O_3	0.2
TiO_2	0.5
Na_2O	0.7
K_2O	0.1
Total	100.0

with 3D micrographs and performing quantitative analysis with a variety of measurement tools. By capturing multiple images while the stage is moving, 3D data capturing and stitching can be performed simultaneously. This makes it possible to view and analyze the target's overall contours. Fig. 4 provides micrographs of the GFRP bar surface profiles.

Surface roughness was calculated according to JIS B 0601: 2001 (ISO 4287: ISO 1997) surface texture parameters as follows:

- GFRP1, GFRP2, and GFRP3 bars have deformed/ribbed, helically deformed, and helically grooved surfaces, respectively. Therefore, the characterization of the surface roughness of these bars was defined by the depth of grooves/deformations and the distance between grooves/deformations.
- Another technique that includes three parameters Ra, Rz, and Rz_{JIS} has been used to define the surface roughness of the sand-coated surface for the GFRP5 bar and the double helical wrap/sand-coated surface for the GFRP4 bar, where Ra is referred to as *Arithmetic mean roughness*, which indicates the average surface roughness of the reference length (i.e., the average difference between peaks and valleys); Rz is called *Maximum roughness*, which indicates the absolute vertical distance between the highest peak and the deepest valley along the reference length; and Rz_{JIS} is referred to as *Ten-point mean roughness*, which represents the sum of the mean value of the height of the five tallest peaks and the mean of the depth of the five deepest valleys of a profile within the reference length.

Table 2 presents the test results of the surface roughness of the tested GFRP bars.

Physical Properties of the GFRP Bars

The physical characterizations of the No. 5 and No. 8 GFRP bars used in this study were determined in accordance with ASTM D7957-22 (ASTM 2022a) and its referenced ASTM standards [ASTM D7205-21 (ASTM 2021a), ASTM D792-20 (ASTM 2020a), ASTM D3171-22 (ASTM 2022b), ASTM D570-98 (ASTM 2018b), ASTM E1356-08 (ASTM 2014), and ASTM E2160-04 (ASTM 2018a)]. Physical tests were conducted to determine the quality of the production process including cross-sectional area, fiber content, moisture absorption, glass transition temperature, and degree of cure.

Cross-Sectional Area and Diameter

Because the section shape and the surface treatments of the GFRP bars did not allow an adequate direct measurement of the dimensions required to calculate the cross-sectional area, the cross-sectional area was calculated with Archimedes' principle of water displacement (volumetric method) in accordance with ASTM D7205-21 (ASTM 2021a) and ASTM D792-20 (ASTM 2020a). Five samples were cut from each GFRP bar type. Laboratory temperature was maintained at 23°C ± 3°C and relative humidity at 50 ± 10% during testing. The maximum diameters of the No. 5 and No. 8 GFRP bars were measured at three different locations using a digital caliper, as shown in Fig. 5.

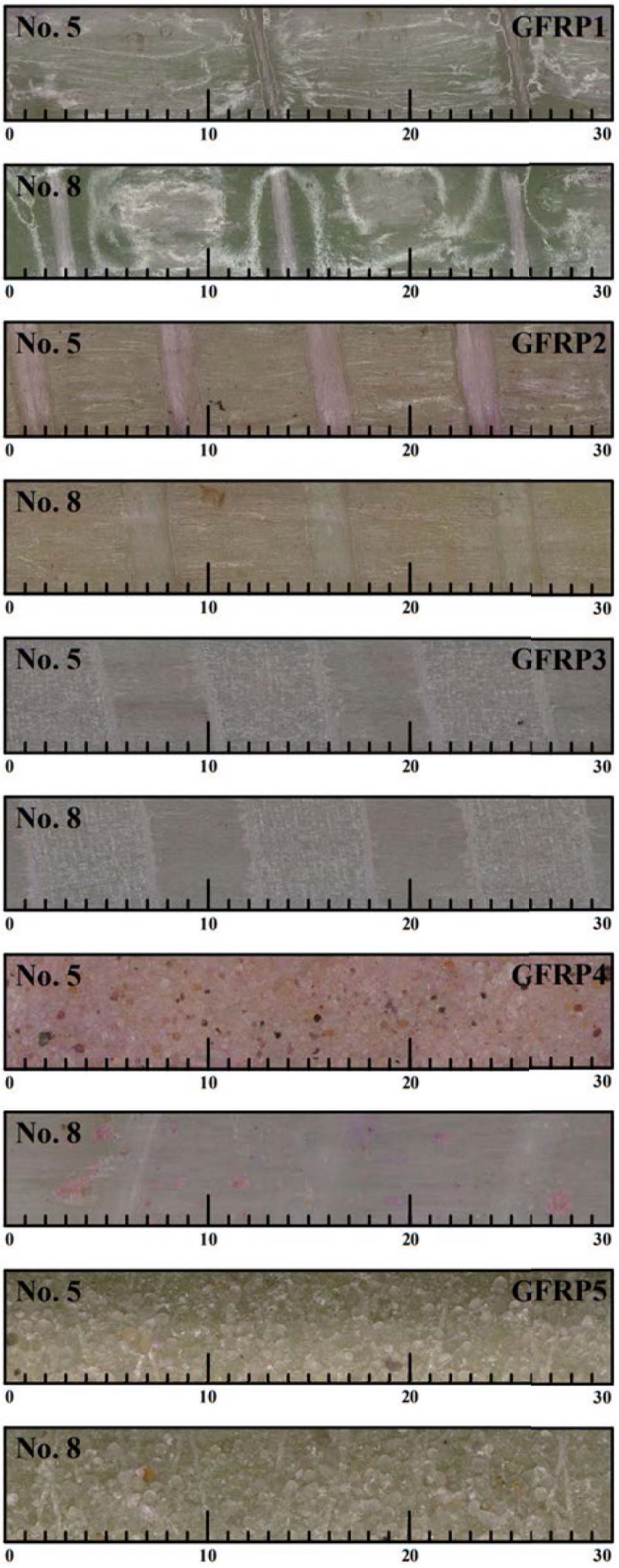

Fig. 4. Surface conditions of the GFRP bars taken with the digital microscope: (1) all GFRP bars are in the horizontal direction; and (2) dimensions in mm).

Table 2. Test results of the surface roughness of the No. 5 and No. 8 GFRP bars

	GFRP1		GFRP2		GFRP3		GFRP4		GFRP5	
Surface texture parameter	No. 5	No. 8	No. 5	No. 8	No. 5	No. 8	No. 5	No. 8	No. 5	No. 8
Depth of grooves/deforms (μm)	960	1,280	600	650	380	200	Not visible[a]	300	—	—
Distance between grooves/deforms (mm)	13.0	11.5	7.5	9.0	11.0	11.0	Not visible[a]	10.0	—	—
Ra (μm)	—	—	—	—	—	—	70	Not enough sand[b]	115	110
Rz (μm)	—	—	—	—	—	—	365	Not enough sand[b]	535	535
Rz_{JIS} (μm)	—	—	—	—	—	—	115	Not enough sand[b]	315	300

[a]The depth of grooves for the No. 5 GFRP4 bar were too small (not visible) to measure. Therefore, the surface roughness of this bar was measured using the data from the sand-coated surface.

[b]As there was not enough sand on the No. 8 GFRP4 bar to use the three-parameter characterization, the surface roughness of this bar was measured using the data from the double helical wrap surface.

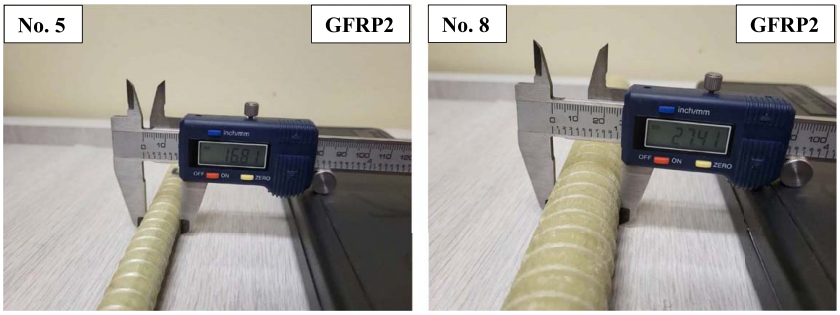

Fig. 5. Measured diameter of the No. 5 and No. 8 GFRP bars.

Fiber Mass Fraction

The fiber mass fraction is considered one of the most important parameters determining the physical and mechanical properties of GFRP bars (ACI 440.1R-15, ACI 2015). Five samples measuring 50 mm in length were cut for each GFRP bar type and diameter. The fiber mass fraction was measured in accordance with ASTM D3171-22 (Method I, Procedure G) (ASTM 2022b). The specimens were weighed (W_T) and heated at 600°C for 6 h to remove the matrix. Thereafter, the glass fiber (W_F), sand (W_S), and wrapping (W_W) weights were determined. The fiber content by weight was calculated by using the following equation:

$$\text{Fiber content by weight (\%)} = \frac{W_F}{W_T - W_S - W_W} \times 100 \quad (1)$$

Moisture Absorption after 24 h and at Saturation

The water absorption of the No. 5 and No. 8 GFRP bars after 24 h and at saturation was determined in accordance with ASTM D570-98 (Procedure 7.1) (ASTM 2018b). Five samples were cut to a length of 50 mm, surface-dried, and weighed prior to immersion in water at 50°C. The specimens were removed from the water after 24 h or more than 3 weeks (corresponding to saturation), dried with a dry cloth, and weighed to the nearest 1×10^{-3} g. The increase in weight (%) was calculated using the following equation:

$$W_{\text{increase}}(\%) = \frac{W_{\text{wet}} - W_{\text{conditioned}}}{W_{\text{conditioned}}} \times 100 \quad (2)$$

where W_{increase} = increase in weight (%); and W_{wet} and $W_{\text{conditioned}}$ = weights of the sample after immersion and prior to immersion, respectively.

Glass Transition Temperature

The glass transition temperature (T_g) was determined in accordance with ASTM E1356-08 (ASTM 2014) with differential scanning calorimetry (DSC). DSC is a rapid test method for determining changes in the specific heat capacity in a material. Its main advantage over other techniques—such as dynamic mechanical analyzing—is the ease and speed with which it can be used to see transitions in materials. The tests were carried out on five samples. The samples were cut from different GFRP bars, with each sample weighing a minimum of 5 mg, weighed, and placed in aluminum pans before being heated from 25°C to 200°C at a rate of 20°C/min.

Degree of Cure

The cure ratio was determined in accordance with ASTM E2160-04 (ASTM 2018a). The enthalpy of polymerization of each specimen was measured by DSC and compared with the enthalpy of polymerization of the pure resin, considering the weight percentage of resin in the matrix. Samples weighing between 30 and 50 mg were cut from different GFRP bars, weighed, and placed in aluminum pans. The samples were then heated from room temperature to 200°C at 20°C/min.

Mechanical Properties of the GFRP Bars

Mechanical characterization included testing the GFRP specimens to determine tensile strength in accordance with ASTM D7205-21 (ASTM 2021a) and CSA S806-12 (CSA 2021) (Annex C), and bond strength by the pullout test in accordance with ASTM D7913-14 (ASTM 2020b). The mechanical properties reported herein were based on nominal cross-sectional areas rather than the measured areas. This is an appropriate approach as the design engineer will not know which bar manufacturer will be selected by the contractor, only that the selected bars must be compliant with ASTM D7957-22 (ASTM 2022a) requirements. ACI 440.11-22 (ACI 2022) also requires the use of nominal bar dimensions when converting from bar force to stress in design.

Tensile Properties of the GFRP Bars

Tensile testing of the GFRP bars was performed by testing five samples for each type. The tests were conducted on GFRP bars with a free length of 40 times the bar diameter ($40d_b$) between steel tube anchors. An expansive cement grout was placed in the tubes to restrain the bar ends. The samples were instrumented with a 200 mm high-accuracy linear variable differential transformer (LVDT) to capture sample elongation in the middle part of the sample between the grips during testing in accordance with ASTM D7205-21 (ASTM 2021a). A Baldwin testing machine was employed to test the bars up to failure. The measured data (applied load and sample elongation) were automatically recorded during the test. The ultimate tensile strength (f_u) of the GFRP bars was estimated from the following equation:

$$f_u = \frac{F_u}{A} \tag{3}$$

where f_u = tensile strength (MPa); F_u = tensile capacity (N); and A = nominal cross-sectional area of the bar (mm^2).

The tensile modulus of elasticity (E_L) of the GFRP bars was estimated from the difference between the load–strain curve values at 25% and 50% of the tensile capacity, as shown in the following equation:

$$E_L = \frac{F_1 - F_2}{(\varepsilon_1 - \varepsilon_2)A} \tag{4}$$

where E_L = tensile modulus of elasticity (MPa); F_1 and F_2 = load (N) at 50% and 25%, respectively, of the ultimate tensile capacity; and ε_1 and ε_2 = corresponding strain to the load at 50% and 25%, respectively, of the ultimate tensile capacity.

Bond Strength of the GFRP Bars (Pullout Test)

Pullout tests were carried out to assess the bond strength of the GFRP bars. The bonded length was kept constant at five times the bar diameter ($5d_b$), where d_b is the nominal bar diameter. The load was applied under load control with a Baldwin loading machine to the surface of the concrete blocks and at a loading rate of 0.1 kN/min. The concrete blocks, which measured 200 mm × 200 mm × 200 mm, were cast with normal-strength concrete with a target concrete strength of 35 MPa. The measured average concrete compressive strength was 41.6 MPa, which was determined on the day of testing from three 100 × 200 mm concrete cylinders in accordance with ASTM C39/C39M-21 (ASTM 2021b). Fig. 6 shows the preparation of the GFRP bars for pullout testing. One LVDT was used to measure the free-end slip of the GFRP bar.

Fig. 6. Preparation of the GFRP bars for pullout testing.

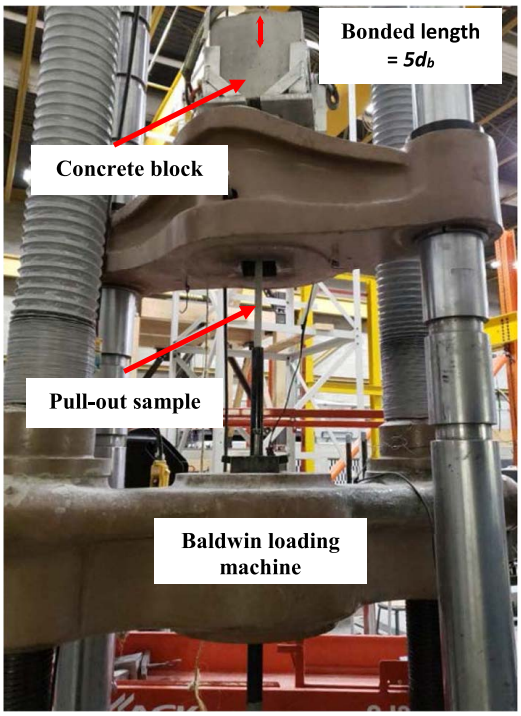

Fig. 7. Typical setup for pullout testing the GFRP bars.

Fig. 7 shows the typical test setup. The pullout bond strength was calculated from the following equation:

$$\tau = \frac{F}{\pi d_b l} \tag{5}$$

where τ = average bond stress (MPa); F = tensile force (N); d_b = nominal bar diameter (mm); and l = bonded length (mm).

Experimental Results and Discussions

Physical Properties of the GFRP Bars

Cross-Sectional Area

Table 3 presents the cross-sectional area for the No. 5 and No. 8 GFRP bars. As the table indicates, all the GFRP bars tested met the requirements of ASTM D7957-22 (ASTM 2022a) and CSA S807-19 (CSA 2019), except No. 5 and No. 8 GFRP1 bars, which had average cross-sectional areas of 259 and 598 mm^2, respectively, slightly greater than the respective maximum limits of 251 and 589 mm^2 in ASTM D7957-22 (ASTM 2022a) and CSA S807-19 (CSA 2019). Cross-sectional areas that are out of compliance with ASTM D7957-22 (ASTM 2022a) are italicized in the table. All of the bars had measured areas well in excess of the nominal areas of 199 and 519 mm^2 for the No. 5 and No. 8 bars, respectively.

Measured and nominal bar diameters are listed in Table 4. As can be seen, the average measured diameters of the No. 5 GFRP bars are greater than the nominal diameter by 17.2%, 5.7%, 5.7%, 11.0%, and 10.2% for GFRP1, GFRP2, GFRP3, GFRP4, and GFRP5, respectively. The same observation for the No. 8 GFRP bars, which had average measured diameters of 28.89, 27.72, 27.26, 28.10, and 27.47 mm for GFRP1, GFRP2, GFRP3, GFRP4, and GFRP5, respectively, indicates that those bars are larger than the nominal diameter by 12.0%, 8.3%, 6.8%, 9.6%, and 7.5%. The issue of oversized bars may result in part from the GFRP bar surface configuration. The grooves/sand-coating/ribs do not contribute to

Table 3. Cross-sectional area of the No. 5 and No. 8 GFRP bars from immersion testing

	Cross-sectional area (mm^2)													
	No. 5							No. 8						
						Limit: min. to max.							Limit: min. to max.	
Specimen no.	GFRP1	GFRP2	GFRP3	GFRP4	GFRP5	ASTM D7957-22	CSA S807-19	GFRP1	GFRP2	GFRP3	GFRP4	GFRP5	ASTM D7957-22	CSA S807-19
1	*261*	236	228	249	238	186 to 251	186 to 251	*604*	582	565	588	558	476 to 589	476 to 589
2	*259*	238	225	248	234			*599*	575	578	576	563		
3	*257*	239	229	247	232			*594*	582	572	586	555		
4	*260*	237	227	243	236			*600*	568	573	579	573		
5	*258*	236	229	249	237			*593*	575	572	589	569		
Average	*259*	237	228	247	235			*598*	576	572	584	564		
SD	1.6	1.3	1.7	2.5	2.4			4.5	5.9	4.6	5.8	7.5		
COV (%)	0.6	0.5	0.7	1.0	1.0			0.8	1.0	0.8	1.0	1.3		

Note: Values in italics exceed the corresponding limits specified in ASTM D7957-22 and CSA S807-19.

the tensile properties of GFRP bars, but are necessary for GFRP bar bond to the concrete (Solyom and Balázs 2020).

An analysis of Table 4 in ASTM D7957-22 (ASTM 2022a) indicates that the maximum allowed measured cross-sectional areas for each bar size correspond to bar diameters that are approximately 2 mm larger than the nominal diameters for bar sizes between No. 2 and No. 9 and about 1.5 mm larger for No. 10 bars, assuming that the bars are perfectly round. This relatively large increase in measured diameter with respect to the nominal diameter (both in the bars investigated in this study and from the limits in ASTM D7957-22) may lead to constructability issues if there is insufficient clear space between the bars to properly place the concrete. ACI 440.11-22 (ACI 2022) currently calls for a clear spacing of the largest of 25.4 mm, d_b, and (4/3) times the aggregate maximum diameter for bars in a single layer. For No. 5 and No. 8 bars using a concrete with a maximum aggregate size of 19.0 mm, the 25.4 mm limit and 4/3 maximum aggregate size limits control simultaneously. As an example, using nominal dimensions, the width of a beam reinforced with four No. 8 bars and a No. 4 stirrup, with a clear cover of 38 mm would be 330 mm. However, if the measured diameters of the stirrup and the No. 8 bars were 2 mm larger than the nominal dimensions, then the resulting clear spacing

Table 4. Diameter of the No. 5 and No. 8 GFRP bars

	Diameter (mm)											
	No. 5						No. 8					
					Nominal diameter						Nominal diameter	
Bar type	Dia. (1)	Dia. (2)	Dia. (3)	Dia. (Ave)	ASTM D7957-22	CSA S807-19	Dia. (1)	Dia. (2)	Dia. (3)	Dia. (Ave)	ASTM D7957-22	CSA S807-19
GFRP1	19.07	19.28	19.28	19.21	15.90	15.90[a]	28.51	28.66	29.50	28.89	25.40	25.40[a]
GFRP2	16.85	16.81	16.95	16.87			27.92	27.41	27.83	27.72		
GFRP3	16.85	16.87	16.90	16.87			27.19	27.32	27.28	27.26		
GFRP4	17.79	17.82	17.99	17.87			28.05	28.14	28.10	28.10		
GFRP5	17.60	17.60	17.96	17.72			27.46	27.56	27.39	27.47		

[a]Nominal diameter was calculated from the nominal cross-sectional area for CSA S807-19 (CSA 2019).

Table 5. Fiber mass fraction of the No. 5 and No. 8 GFRP bars

	Fiber mass fraction (%)													
	No. 5							No. 8						
						Limit							Limit	
Specimen no.	GFRP1	GFRP2	GFRP3	GFRP4	GFRP5	ASTM D7957-22	CSA S807-19	GFRP1	GFRP2	GFRP3	GFRP4	GFRP5	ASTM D7957-22	CSA S807-19
1	79.9	82.0	83.0	84.1	84.2	≥70.0	≥70.0	79.4	82.9	82.1	84.2	82.5	≥70.0	≥70.0
2	79.7	81.9	83.0	84.2	84.1			79.3	82.8	82.1	84.1	82.6		
3	79.9	81.9	83.1	84.3	84.1			79.4	83.0	82.0	84.0	82.7		
4	79.8	81.8	83.1	84.1	84.0			79.3	83.0	82.1	84.1	82.6		
5	79.9	81.8	83.1	84.2	84.1			79.3	82.9	82.1	84.1	82.7		
Average	79.8	81.9	83.0	84.2	84.1			79.3	82.9	82.1	84.1	82.6		
SD	0.1	0.1	0.1	0.1	0.1			0.1	0.1	0.0	0.1	0.1		
COV (%)	0.1	0.1	0.1	0.1	0.1			0.1	0.1	0.1	0.1	0.1		

Table 6. Short-term moisture absorption of the No. 5 and No. 8 GFRP bars at 24 h

	Short-term moisture absorption (%)													
	No. 5							No. 8						
						Limit							Limit	
Specimen no.	GFRP1	GFRP2	GFRP3	GFRP4	GFRP5	ASTM D7957-22	CSA S807-19	GFRP1	GFRP2	GFRP3	GFRP4	GFRP5	ASTM D7957-22	CSA S807-19
1	*0.26*	0.08	0.03	0.21	0.05	≤0.25	≤0.25	0.06	0.03	0.01	0.09	0.09	≤0.25	≤0.25
2	*0.23*	0.07	0.01	0.22	0.06			0.06	0.03	0.01	0.09	0.11		
3	*0.32*	0.05	0.03	0.20	0.06			0.06	0.03	0.01	0.10	0.12		
4	*0.30*	0.06	0.01	0.21	0.05			0.06	0.02	0.01	0.10	0.09		
5	0.22	0.07	0.02	0.25	0.05			0.06	0.03	0.01	0.10	0.13		
Average	*0.27*	0.07	0.02	0.22	0.05			0.06	0.03	0.01	0.10	0.10		
SD	0.04	0.01	0.01	0.02	0.01			0.00	0.00	0.00	0.01	0.02		
COV (%)	16.3	17.3	50.0	8.8	10.1			0.0	16.0	0.0	5.7	16.6		

Note: Values in italics exceed the corresponding limits specified in ASTM D7957-22 and CSA S807-19.

in that same 330 mm diameter wide beam would be 18.0 mm, which is less than the maximum aggregate size. Such a beam would not be constructible as designed. Two possible solutions exist to correct this potential problem: (1) ACI 440.11-22 (ACI 2022) could increase the required clear spacing between bars by 2 mm, or (2) ASTM D7957-22 (ASTM 2022a) could tighten the requirements on measured cross-sectional areas in Table 3. The second alternative would have significant implications for manufacturers on meeting other requirements such as stiffness. Designers and engineers should consider this issue when they are calculating bar placement in engineering drawings, as the clear spacing between bars currently required by ACI 440.11-22 (ACI 2022) may not be sufficient for the concrete to flow easily.

Fiber Mass Fraction

Table 5 presents the fiber mass fraction for the No. 5 and No. 8 GFRP bars. The test results indicate that all the tested GFRP bars had high fiber mass fractions. The average fraction was between 79.8% and 84.2% for the No. 5 GFRP bars and between 79.3% and 84.1% for the No. 8 GFRP bars. These results easily satisfy the 70% minimum requirements of ASTM D7957-22 (ASTM 2022a) and CSA S807-19 (CSA 2019).

Table 7. Moisture absorption of the No. 5 and No. 8 GFRP bars at saturation

	Moisture absorption at saturation (%)													
	No. 5							No. 8						
						Limit							Limit	
Specimen no.	GFRP1	GFRP2	GFRP3	GFRP4	GFRP5	ASTM D7957-22	CSA S807-19	GFRP1	GFRP2	GFRP3	GFRP4	GFRP5	ASTM D7957-22	CSA S807-19
1	0.45	0.20	0.05	0.66	0.26	≤1.00	<0.75	0.21	0.12	0.04	0.32	0.14	≤1.00	<0.75
2	0.44	0.20	0.04	0.64	0.17			0.21	0.11	0.05	0.32	0.13		
3	0.45	0.20	0.04	0.61	0.22			0.21	0.11	0.04	0.32	0.20		
4	0.47	0.19	0.03	0.57	0.27			0.20	0.12	0.04	0.33	0.17		
5	0.48	0.18	0.08	0.58	0.21			0.21	0.12	0.04	0.35	0.17		
Average	0.45	0.19	0.05	0.61	0.22			0.21	0.12	0.04	0.33	0.16		
SD	0.02	0.01	0.02	0.04	0.04			0.00	0.01	0.00	0.01	0.03		
COV (%)	3.6	4.6	40.1	6.3	17.9			2.2	4.7	10.6	4.0	17.1		

Table 8. Glass transition temperature (T_g) of the No. 5 and No. 8 GFRP bars

	T_g (°C)													
	No. 5							No. 8						
						Limit							Limit	
Specimen no.	GFRP1	GFRP2	GFRP3	GFRP4	GFRP5	ASTM D7957-22	CSA S807-19	GFRP1	GFRP2	GFRP3	GFRP4	GFRP5	ASTM D7957-22	CSA S807-19
1	113	127	113	108	112	≥100	≥100	103	126	113	111	120	≥100	≥100
2	114	125	112	106	112			104	125	114	110	119		
3	115	129	113	105	113			105	126	116	110	117		
4	116	125	112	107	111			104	126	114	110	120		
5	114	125	112	109	110			105	126	114	113	118		
Average	114	126	112	107	112			104	126	114	111	119		
SD	1.1	1.8	0.5	1.6	1.1			0.8	0.4	1.1	1.3	1.3		
COV (%)	1.0	1.4	0.5	1.5	1.0			0.8	0.4	1.0	1.2	1.1		

J. Compos. Constr., 2023, 27(6): 04023056

Table 9. Degree of cure of the No. 5 and No. 8 GFRP bars

	Degree of cure (%)													
	No. 5							No. 8						
						Limit							Limit	
Specimen no.	GFRP1	GFRP2	GFRP3	GFRP4	GFRP5	ASTM D7957-22	CSA S807-19	GFRP1	GFRP2	GFRP3	GFRP4	GFRP5	ASTM D7957-22	CSA S807-19
1	98	100	97	99	96	≥95	≥95	*95*	100	100	98	96	≥95	≥95
2	97	100	97	99	97			*93*	100	100	98	98		
3	98	100	97	98	95			96	100	100	97	95		
4	97	100	96	99	95			*94*	100	100	98	97		
5	98	100	98	98	96			*94*	100	100	98	95		
Average	98	100	97	99	96			*94*	100	100	98	96		
SD	0.5	0.0	0.7	0.5	0.8			1.1	0.0	0.0	0.4	1.3		
COV (%)	0.6	0.0	0.7	0.6	0.9			1.2	0.0	0.0	0.5	1.4		

Note: Values in italics exceed the corresponding limits specified in ASTM D7957-22 and CSA S807-19.

Moisture Absorption after 24 h and at Saturation

Water absorption limits have been established as a means for quickly identifying manufacturing-line problems, particularly related to porosity, which can adversely affect adequate durability of GFRP mechanical bar properties. Tables 6 and 7 present the water absorption of the No. 5 and No. 8 GFRP bars after 24 h and at saturation, respectively, which show that the water absorption after 24 h ranged from 0.02% to 0.27% for the No. 5 GFRP bars and from 0.01% to 0.10% for the No. 8 GFRP bars, on average, based on five samples of each GFRP bar type. These values fall within the limits specified in ASTM D7957-22 (ASTM 2022a) and CSA S807-19 (CSA 2019) (0.25%), except for the GFRP1 bars, which had an average water absorption of 0.27% (>0.25%). Values not meeting the limits of ASTM D7957-22 (ASTM 2022a) are italicized in Table 6. The water absorption at saturation ranged from 0.05% to 0.61% for the No. 5 GFRP bars and 0.04% to 0.33% for the No. 8 GFRP bars, on average, based on five samples for each GFRP bar type. These values fall within the limits specified in ASTM D7957-22 (ASTM 2022a) (1.00%) and CSA S807-19 (CSA 2019) (0.75%).

Glass Transition Temperature

Table 8 provides the glass transition temperature T_g of all the tested bars. As shown, the average T_g for the No. 5 and No. 8 GFRP bars ranged from 107°C to 126°C and from 104°C to 126°C, respectively. The comparison between the test results and the specified limit of 100°C for DSC technique in ASTM D7957-22 (ASTM 2022a) and CSA S807-19 (CSA 2019) confirms that all GFRP bars tested met the requirements of the ASTM specification.

Degree of Cure

As proposed by manufacturers, a typical value of (250 J/g) for the enthalpy of polymerization of the vinyl-ester resin was used to estimate the cure ratio for all types of GFRP bars. Establishing a minimum degree of resin cure for a GFRP bar is another way to guarantee the durability of the product. The average cure ratios for the No. 5 GFRP bars ranged from 96% to 100%, which are higher than the 95% required in ASTM D7957-22 (ASTM 2022a) and CSA S807-19 (CSA 2019). The average cure ratios for the No. 8 GFRP bars exceeded the 95% recommended in ASTM D7957-22 (ASTM 2022a) and CSA S807-19 (CSA 2019), except for the GFRP1 bars, which had an average degree of cure of 94%. Table 9 presents the summary of the curing-ratios results with values that do not meet the requirements of ASTM D7957-22 (ASTM 2022a) italicized.

Fig. 8. Typical mode of tensile failure of the GFRP bars (No. 5 and No. 8).

Mechanical Properties of GFRP Bars

Tensile Properties of the GFRP Bars

The tested samples show linear elastic behavior up to failure. All samples failed suddenly because of tensile fiber rupture. The No. 5 and No. 8 GFRP bars exhibited high tensile strength that met the ASTM D7957-22 (ASTM 2022a) requirements for No. 5 and No. 8 GFRP bars of 653 and 582 MPa, respectively. In addition, types GFRP1, GFRP2, GFRP3, GFRP4, and GFRP5 had an average tensile moduli of elasticity of 63, 64, 60, 62, and 62 GPa, respectively, for the No. 5 GFRP bars and 60, 63, 61, 62, and 61 GPa, respectively, for the No. 8 GFRP bars, which correspond to Grade III (GIII) for GFRP bars according to the CSA S807-19 (CSA 2019) classification (modulus of elasticity of 60 GPa). The average tensile moduli of elasticity for the No. 5 and No. 8 GFRP bars greatly exceed the requirements of GFRP bars according to ASTM D7957-22 (ASTM 2022a) (44.8 GPa). Moreover, the tested samples had average tensile strains at failure for the No. 5 and No. 8 GFRP bars that ranged from 1.7% to 2.4% and from 1.3% to 1.9%, respectively. These values are larger than the 1.1% and 1.2% in ASTM D7957-22 (ASTM 2022a) and CSA S807-19 (CSA 2019) provisions, respectively. Fig. 8 presents the typical mode of tensile failure of the GFRP bars. Tables 10–14 present the tensile properties of the GFRP samples, while Table 15 presents the specified limits for longitudinal tensile properties of No. 5 and No. 8 GFRP bars.

Table 16 shows the manufacturer's guaranteed values for the tensile strengths of No. 5 and No. 8 GFRP bars. Values in Tables 10–14 that were below the manufacturer's guaranteed values are italicized. The average tensile strengths of GFRP bars in this study were higher than the manufacturer's guaranteed values, with the exception of No. 8 GFRP2, GFRP3, and GFRP5 bars.

Table 10. Longitudinal tensile properties of the GFRP1 bars (No. 5 and No. 8)

	No. 5				No. 8			
Specimen no.	Ultimate load (kN)	Tensile strength (MPa)	Tensile modulus (GPa)	Ultimate strain (%)	Ultimate load (kN)	Tensile strength (MPa)	Tensile modulus (GPa)	Ultimate strain (%)
1	270	1,359	62	2.2	599	1,174	60	2.0
2	235	1,180	61	1.9	569	1,115	60	1.9
3	238	1,196	63	1.9	568	1,114	61	1.8
4	262	1,316	65	2.0	550	1,079	60	1.8
5	254	1,276	62	2.1	595	1,167	60	1.9
Average	252	1,265	63	2.0	576	1,130	60	1.9
SD	15.1	76.7	1.5	0.1	20.5	40.0	0.4	0.1
COV (%)	6.0	6.1	2.4	6.5	3.6	3.5	0.7	4.5

Table 11. Longitudinal tensile properties of the GFRP2 bars (No. 5 and No. 8)

	No. 5				No. 8			
Specimen no.	Ultimate load (kN)	Tensile strength (MPa)	Tensile modulus (GPa)	Ultimate strain (%)	Ultimate load (kN)	Tensile strength (MPa)	Tensile modulus (GPa)	Ultimate strain (%)
1	278	1,397	61	2.3	546	1,071	62	1.7
2	267	1,342	64	2.1	537	1,053	64	1.6
3	303	1,523	65	2.4	524	1,027	63	1.6
4	291	1,462	65	2.3	464	*910*	62	1.5
5	276	1,387	64	2.2	473	*927*	64	1.4
Average	283	1,422	64	2.3	509	*998*	63	1.6
SD	14.1	70.8	1.6	0.1	37.7	74.1	1.0	0.1
COV (%)	5.0	5.0	2.6	5.0	7.4	7.4	1.6	7.3

Note: Values in italics do not meet minimum requirements of CSA S807-19 and were less than the manufacturer's guaranteed value.

Table 12. Longitudinal tensile properties of the GFRP3 bars (No. 5 and No. 8)

	No. 5				No. 8			
Specimen no.	Ultimate load (kN)	Tensile strength (MPa)	Tensile modulus (GPa)	Ultimate strain (%)	Ultimate load (kN)	Tensile strength (MPa)	Tensile modulus (GPa)	Ultimate strain (%)
1	199	1,001	59	1.7	401	*786*	62	1.3
2	183	*921*	60	1.5	399	*782*	60	1.3
3	200	1,007	60	1.7	411	*807*	61	1.3
4	216	1,083	63	1.7	426	*836*	62	1.4
5	201	1,009	61	1.7	406	*796*	61	1.3
Average	200	1,004	60	1.7	409	*801*	61	1.3
SD	11.7	57.4	1.5	0.1	10.8	21.6	0.8	0.0
COV (%)	5.9	5.7	2.5	5.4	2.6	2.7	1.4	3.4

Note: Values in italics do not meet minimum requirements of CSA S807-19 and were less than the manufacturer's guaranteed value.

Table 13. Longitudinal tensile properties of the GFRP4 bars (No. 5 and No. 8)

	No. 5				No. 8			
Specimen no.	Ultimate load (kN)	Tensile strength (MPa)	Tensile modulus (GPa)	Ultimate strain (%)	Ultimate load (kN)	Tensile strength (MPa)	Tensile modulus (GPa)	Ultimate strain (%)
1	262	1,318	61	2.1	530	1,040	61	1.7
2	250	1,254	61	2.1	551	1,081	61	1.8
3	253	1,269	61	2.1	539	1,058	62	1.7
4	251	1,261	63	2.0	551	1,080	63	1.7
5	259	1,302	61	2.1	553	1,083	62	1.7
Average	255	1,281	62	2.1	545	1,068	62	1.7
SD	5.2	27.8	0.9	0.04	10.0	18.8	0.8	0.05
COV (%)	2.1	2.2	1.5	1.9	1.8	1.8	1.4	2.9

The No. 5 GFRP3 bars also had a single test value that was below the manufacturer's guaranteed value. ASTM D7957-22 defines the manufacturer's guaranteed strength as a value no larger than the mean minus three standard deviations of at least 24 samples in groups of eight or more from three or more production lots. If the manufacturer's guaranteed value is reflective of the population mean minus three standard deviations, then the probability of a single test being below the manufacturer's guaranteed strength value

Table 14. Longitudinal tensile properties of the GFRP5 bars (No. 5 and No. 8)

	No. 5				No. 8			
Specimen no.	Ultimate load (kN)	Tensile strength (MPa)	Tensile modulus (GPa)	Ultimate strain (%)	Ultimate load (kN)	Tensile strength (MPa)	Tensile modulus (GPa)	Ultimate strain (%)
1	292	1,469	63	2.3	519	*1,017*	61	1.7
2	299	1,502	62	2.4	539	*1,056*	61	1.7
3	306	1,535	62	2.5	535	*1,049*	62	1.7
4	306	1,538	62	2.5	561	1,100	61	1.8
5	294	1,475	62	2.4	514	*1,008*	61	1.6
Average	299	1,504	62	2.4	534	*1,046*	61	1.7
SD	6.5	32.4	0.3	0.1	18.5	36.2	0.5	0.1
COV (%)	2.2	2.2	0.6	3.5	3.5	3.5	0.7	4.2

Note: Values in italics were less than the manufacturer's guaranteed value.

Table 15. Specified limits of longitudinal tensile properties of the GFRP bars (No. 5 and No. 8)

	No. 5		No. 8	
Property	ASTM D7957-22	CSA S807-19	ASTM D7957-22	CSA S807-19
Ultimate load (kN)	≥130	—	≥297	—
Tensile strength (MPa)	—	≥1,000	—	≥1,000
Tensile modulus (GPa)	≥44.8	≥60.0	≥44.8	≥60.0
Ultimate strain (%)	≥1.1	≥1.2	≥1.1	≥1.2

Table 16. Manufacturer-reported modulus of elasticity and manufacturer-guaranteed tensile strength values of the GFRP bars (No. 5 and No. 8)

	No. 5					No. 8				
Property	GFRP1	GFRP2	GFRP3	GFRP4	GFRP5	GFRP1	GFRP2	GFRP3	GFRP4	GFRP5
Modulus of elasticity (GPa)	60.0	63.0	60.0	62.6	60.0	60.0	63.0	60.0	61.7	60.0
Guaranteed tensile strength (MPa)	>1,000	>1,200	≥1,000	1,150	1,100	>1,000	>1,000	≥889	1,000	1,100

Fig. 9. Bond failure of the GFRP1 bars.

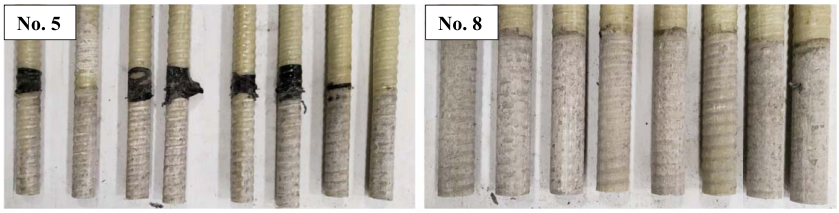

Fig. 10. Bond failure of the GFRP2 bars.

is 0.135%. As ASTM D7957 is currently written, if these bars had been tested for a project none of the bars would have been rejected. ASTM D7957-22 (ASTM 2022a) Section 11 states that "for quality control and certification, if a single test result from five samples selected randomly from each production lot is not within the limits given … (i.e., ultimate tensile force larger than the minimum guaranteed ultimate tensile force) that production lot shall be rejected as not meeting this specification." This is clearly a shortcoming of ASTM D7957-22. Rejection should be based on the strength assumed for design, which could be between the minimum specified in ASTM D7957-22 and the manufacturer's guaranteed value. Until ASTM D7957 bases rejection on the strength used in design, the designer should add rejection criteria to the project specifications to require that the bar shipment lot be rejected if a single

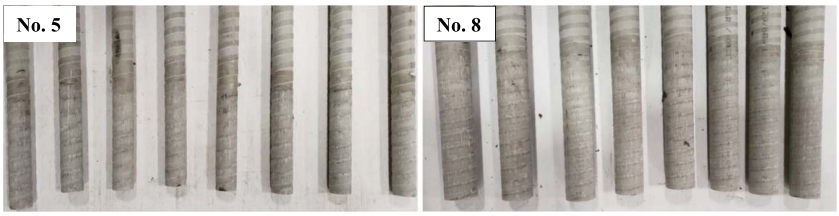

Fig. 11. Bond failure of the GFRP3 bars.

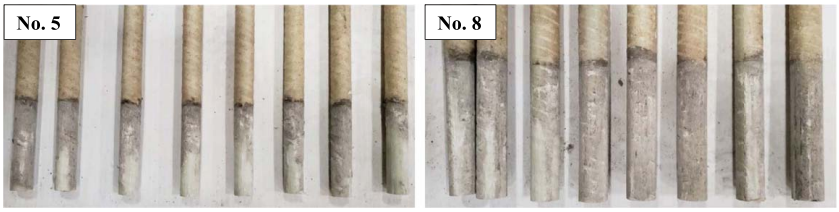

Fig. 12. Bond failure of the GFRP4 bars.

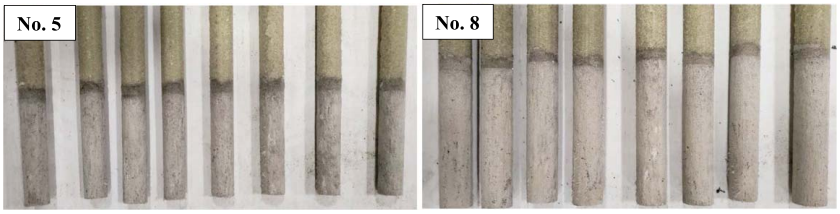

Fig. 13. Bond failure of the GFRP5 bars.

Fig. 14. Bond failure of the steel bars.

Table 17. Bond strength of the No. 5 GFRP and 15 M steel bars

	Bond strength (MPa)							
							Limit	
Specimen no.	GFRP1	GFRP2	GFRP3	GFRP4	GFRP5	Steel	ASTM D7957-22	CSA S807-19
1	26.4	24.2	19.4	11.2	15.9	28.9	≥7.6	≥10.0
2	22.7	23.5	18.5	10.0	16.1	26.7		
3	24.1	22.5	17.3	11.5	15.6	28.5		
4	22.6	21.6	18.4	12.5	19.1	28.6		
5	20.7	22.5	17.2	12.4	14.8	24.3		
6	23.5	20.0	16.3	11.7	18.5	22.7		
7	23.4	21.2	17.6	13.6	18.6	25.7		
8	26.3	20.8	19.2	12.2	18.4	22.7		
Average	23.7 (18.0)[a]	22.0 (17.8)[a]	18.0 (14.7)[a]	11.9 (8.6)[a]	17.1 (12.0)[a]	26.0 (18.2)[a]		
SD	1.9	1.4	1.1	1.1	1.7	2.6		
COV (%)	8.1	6.3	5.9	9.1	9.8	9.9		

[a]Guaranteed bond strength calculated as the mean strength minus three times the standard deviation (ASTM D7957-22, ASTM 2022a).

Table 18. Bond strength of the No. 8 GFRP and 25 M steel bars

	Bond strength (MPa)							
							Limit	
Specimen no.	GFRP1	GFRP2	GFRP3	GFRP4	GFRP5	Steel	ASTM D7957	CSA S807
1	17.2	—[a]	11.4	10.5	12.7	18.6		
2	18.5	—[a]	11.0	9.4	10.3	20.8		
3	16.2	16.7	10.9	11.3	10.5	—[a]		
4	16.4	17.0	11.7	9.6	9.8	19.8		
5	16.3	16.9	11.6	10.9	11.2	19.2		
6	17.9	17.2	11.4	10.3	11.0	19.7	≥7.6	≥10.0
7	16.1	—[a]	11.3	9.6	12.1	19.7		
8	18.3	16.7	11.6	10.8	10.4	20.7		
Average	17.1 (14.1)[b]	16.9 (16.3)[b]	11.4 (10.5)[b]	10.3 (8.5)[b]	11.0 (8.0)[b]	19.9 (17.5)[b]		
SD	1.0	0.2	0.3	0.6	1.0	0.8		
COV (%)	5.8	1.3	2.5	6.0	9.5	3.9		

[a]The sample failed by concrete splitting.
[b]Guaranteed bond strength calculated as the mean strength minus three times the standard deviation (ASTM D7957-22, ASTM 2022a).

test result from five samples selected randomly from the shipment is below the strength value used in design.

Bond Strength of the GFRP Bars (Pullout Test)

Figs. 9–14 present the bond failure of the GFRP and steel bars. All specimens failed by bar slip (shearing of the annulus of concrete surrounding the bar deformations was observed with almost no damage to the GFRP bars), except Specimen no. 3 of the 25 M steel bars and three specimens of the No. 8 GFRP2 bars (Specimen nos. 1, 2, and 7), which failed by concrete splitting. Tables 17 and 18 give the bond strengths of the tested GFRP and steel bars. As can be seen, GFRP1, GFRP2, GFRP3, GFRP4, and GFRP5 bars exhibited an average bond strength of 23.7, 22.0, 18.0, 11.9, and 17.1 MPa, respectively, for the No. 5 GFRP bars and 17.1, 17.0, 11.4, 10.3, and 11.0 MPa, respectively, for the No. 8 GFRP bars. These values exceed the limit of 10.0 MPa specified in CSA S807-19 (CSA 2019). The guaranteed bond strengths of the tested GFRP bars were higher than that required in ASTM D7957-22 (ASTM 2022a) (7.6 MPa). On the other hand, the 15 and 25 M steel bars had average bond strengths of 26.0 and 19.9 MPa, respectively. Therefore, the five types of GFRP bars presented, on average, lower bond strength than the steel bars under the same experimental conditions.

Fig. 15 shows the correlation between surface roughness measurements and bond strength for GFRP bars with grooves. As can be seen, the deeper the groove, the stronger the bond strength, especially for No. 5 GFRP bars. For No. 8 GFRP bars, the difference in bond strength between GFRP1 bars and GFRP2 bars is small, but the difference in groove depth is large. Similarly, for GFRP bars with sand coating (GFRP4 and GFRP5 bars), the results showed that the GFRP bars with the highest bond strength (GFRP5 bars) have higher Ra, Rz, and Rz_{JIS}. In addition, even for the No. 5 GFRP4 bars that have a surface covered with sand of a smaller grain size or insufficient sand as for the No. 8 GFRP4 bars, the average bond strength is still higher than that required in specifications. The reason behind this is that GFRP4 bars have a surface formed by the combination of two conditions (sand coating and double helical wrap). Solyom and Balázs (2020) reported a similar observation for GFRP bars coated by crushed sand in addition to the helical wrapping.

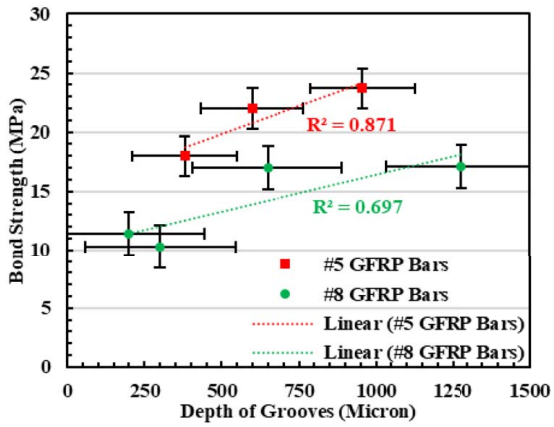

Fig. 15. Bond strength versus depth of grooves for the GFRP bars with grooves.

Conclusions

This research study investigated the physical properties, longitudinal tensile properties, and bond strength of a new generation of GFRP bars. Five different types of GFRP bars with different surface conditions (deformed/ribbed, helically deformed, helically grooved, double helical wrap/sand-coated, and sand-coated) were selected for this investigation. Two diameters of GFRP bars (Nominal no. 5 and no. 8)—representing the range of GFRP-reinforcing bars used in practice as longitudinal reinforcement in concrete members subjected to bending—were selected from each of the manufacturers. Based on the results of this study, the following conclusions have been drawn:

1. Test results of the physical properties of the new generation of GFRP bars show that samples met the requirements in ASTM D7957-22 (ASTM 2022a) and CSA S807-19 (CSA 2019), with the exception of GFRP1 bars with respect to cross-sectional area, water absorption after 24 h, and cure ratio.
2. The difference between measured and nominal cross-sectional areas (and thus diameters) could impact constructability. The maximum cross-sectional areas in ASTM D7957-22 (ASTM 2022a) should be tightened, or the clear spacing limits in ACI 440.11-22 (ACI 2022) should be modified to account for the difference in nominal and measured bar dimensions.
3. Test results indicated that the selected GFRP bars (No. 5 and No. 8) meet the requirements in ASTM D7957-22 (ASTM 2022a) and CSA S807-19 (CSA 2019) with respect to the tensile

properties and bond strength. The measured tensile strength and elastic modulus for these new higher modulus GFRP bars exceeded the requirements of ASTM D7957-22 (ASTM 2022a) and CSA S807-19 (CSA 2019).

4. According to CSA S807-19 (CSA 2019) classification, the tested No. 5 and No. 8 GFRP bars are Grade III (GIII) with a modulus of elasticity equal to or greater than 60 GPa.
5. ASTM D7957-22 (ASTM 2022a) stipulates the minimum characteristics of the GFRP bar to be used in structural elements, which could differ from the values implemented in the design. GFRP bar manufacturers have developed and are producing new generations of GFRP bars with guaranteed strengths that significantly exceed the ASTM D7957-22 (ASTM 2022a) minimum specifications. Therefore, designers/owners/contractors need to ensure that construction documents show the required GFRP bar specifications and rejection requirements for the project. Chapter 26 of ACI 440.11-22 (ACI 2022) establishes the minimum requirements for information that must be included in the construction documents as applicable to the project. Article 26.6.1.1(b) requires the construction documents to show the minimum values for guaranteed ultimate tensile force and tensile modulus of elasticity. Therefore, it is recommended that the prepared quality control and certification report correlates the results to the project specifications shown in the construction documents and not just with the minimum values in ASTM D7957-22 (ASTM 2022a).
6. The bond strength can vary within wide limits for a given surface finish. For GFRP bars with grooves, the deeper the groove, the stronger the bond strength. For sand-coated bars, the bond strength is affected by sand grain size.

Data Availability Statement

All data, models, and code generated or used during the study appear in the published article.

Acknowledgments

The research presented herein was funded by the Natural Sciences and Engineering Research Council of Canada (NSERC). The donation of GFRP bars by Owens Corning (Concord, NC, USA), Pultrall Inc. (Thetford Mines, QC, Canada), B&B FRP Manufacturing Inc. (Toronto, ON, Canada), TUFBAR Canada Inc. (Edmonton, AB, Canada) and ASA.TEC GMBH (Langenlois, Austria) to support this investigation is greatly appreciated. The authors would like to express their special thanks to Jerome Lacroix, Pascal St-Laurent, and Steven MacEachern, technicians in the Department of Civil Engineering at the University of Sherbrooke, for their help during the casting and testing of the GFRP bars (tensile and pullout tests).

References

ACI (American Concrete Institute). 2015. *Guide for the design and construction of concrete reinforced with FRP bars*. ACI 440.1R-15. Farmington Hills, MI: ACI.

ACI (American Concrete Institute). 2022. *Building code requirements for structural concrete reinforced with glass fiber-reinforced polymer (GFRP) bars—Code and commentary*. ACI 440.11-22. Farmington Hills, MI: ACI.

ASTM. 2014. *Standard test method for assignment of the glass transition temperatures by differential scanning calorimetry*. ASTM E1356-08. West Conshohocken, PA: ASTM.

ASTM. 2018a. *Standard test method for heat of reaction of thermally reactive materials by differential scanning calorimetry*. ASTM E2160-04. West Conshohocken, PA: ASTM.

ASTM. 2018b. *Standard test method for water absorption of plastics; procedure 7.1, 24-hour immersion at 122°F*. ASTM D570-98. West Conshohocken, PA: ASTM.

ASTM. 2020a. *Standard test methods for density and specific gravity (relative density) of plastics by displacement*. ASTM D792-20. West Conshohocken, PA: ASTM.

ASTM. 2020b. *Standard test method for bond strength of fiber-reinforced polymer matrix composite bars to concrete by pull-out testing*. ASTM D7913M-14. West Conshohocken, PA: ASTM.

ASTM. 2021a. *Standard test method for tensile properties of fiber reinforced polymer matrix composite bars*. ASTM D7205-21. West Conshohocken, PA: ASTM.

ASTM. 2021b. *Standard test method for compressive strength of cylindrical concrete specimens*. ASTM C39M-21. West Conshohocken, PA: ASTM.

ASTM. 2022a. *Standard specification for solid round glass fiber reinforced polymer bars for concrete reinforcement*. ASTM D7957M-22. West Conshohocken, PA: ASTM.

ASTM. 2022b. *Standard test methods for constituent content of composite materials, method I; procedure G*. ASTM D3171-22. West Conshohocken, PA: ASTM.

Benmokrane, B., and H. Rahman. 1998. "Durability of Fiber-Reinforced Polymer (FRP) composites for construction." In *Proc., 2nd Int. Conf. (CDCC'98)*. Sherbrooke, QC: University of Sherbrooke.

Benmokrane, B., P. Wang, T. M. Ton-That, H. Rahman, and J.-F. Robert. 2002. "Durability of glass fiber-reinforced polymer reinforcing bars in concrete environment." *J. Compos. Constr.* 6 (3): 143–153. https://doi.org/10.1061/(ASCE)1090-0268(2002)6:3(143).

CSA (Canadian Standards Association). 2019. *Specification for fibre-reinforced polymers*. CSA S807-19. Rexdale, ON, Canada: CSA.

CSA (Canadian Standards Association). 2021. Re-approved in 2017—*Design and construction of building components with fiber reinforced polymers*. CSA S806-12. Rexdale, ON, Canada: CSA.

JIS B 0601:. 2001. (ISO 4287: 1997) "Geometrical Product Specifications (GPS)-Surface texture: Profile Method-Terms, Definitions and surface texture parameters." Japanese Industrial Standard.. Rexdale, ON, Canada: CSA.

ISO (International Organization for Standardization). 1997. *Geometrical product specifications (GPS)-surface texture: Profile method-terms, definitions and surface texture parameters*. JIS B 0601: 2001 (ISO 4287: 1997). Tokyo, Japan:: Japanese Industrial Standard.

Micelli, F., and A. Nanni. 2004. "Durability of FRP rods for concrete structures." *Constr. Build. Mater.* 18 (7): 491–503. https://doi.org/10.1016/j.conbuildmat.2004.04.012.

Solyom, S., and G. L. Balázs. 2020. "Bond of FRP bars with different surface characteristics." *Constr. Build. Mater.* 264: 119839. https://doi.org/10.1016/j.conbuildmat.2020.119839.

Tannous, F. E., and H. Saadatmanesh. 1999. "Durability of AR glass fiber reinforced plastic bars." *J. Compos. Constr.* 3 (1): 12–19. https://doi.org/10.1061/(ASCE)1090-0268(1999)3:1(12).

The Digital Microscope VHX-7000. "Keyence digital microscope publication." *KEYENCE's Internal Research/Evaluation, Ontario, Canada*. Accessed February 3, 2023. https://www.keyence.ca/products/microscope/digital-microscope/vhx-7000/index_pr.jsp.

Uomoto, T. 2003. "Durability design of GFRP rods for concrete reinforcement." In Vol. 2 of *Proc., 6th Int. Symp. on FRP Reinforcement for Concrete Structures*, 37–50. Singapore: World Scientific.

Uomoto, T., and F. Katsuki. 1995. "Prediction of deterioration of FRP rods due to alkali attack, non-metallic (FRP) reinforced for concrete structures." In *Proc., 2nd Int.* RILEM Symp. (FRPRCS-2). Ghent, Belgium: Universiteit Ghent.